SUPPLEMENTARY MATERIAL

SUPPLEMENTARY TEXT

The following geodata were used to determine the landslide and debris flow trajectories:

- A grid-based terrain model (DTM) of the whole of Switzerland with 10-meter resolution (Schneider, 1998). The DTM was used to calculate slope inclination, exposure, Topo-Index (Quinn et al., 1995), stream network, gullies, and catchment area.
- The Hydrological Atlas of Switzerland (HADES Sheet 2.4; Geiger et al., 1992) provided a digital map for extreme point rainfall intensities (24 hours duration for a 100-year return period), categorized in three intensity classes (< 150 mm, 150-200 mm, > 200 mm). These values were used as a rough approximation of the critical water content in a given soil (pore water pressure/cohesion).
- Based on the digital geotechnical map of Switzerland (1:200'000), lithological units were classified and attributed with respect to their weatherability and stability (soil resistance against failure) and used for landslide and debris flow modelling.

The simulation of debris flow processes in SilvaProtect-CH was carried out with the model package MGSIM (Zimmermann et al., 1997). Critical slope for debris flow initiation was defined as a function of catchment area according to Zimmermann et al. (1997); the smaller the catchment area above a channel section, the steeper the channel section must be in order for debris flows to occur. The run-out distance of debris flows was estimated using a 2-parameter mass point model based on the Voellmy avalanche model (Gamma, 2000; Perla et al., 1980; Rickenmann, 2005). For given channel reach slopes and friction parameters, the model calculates the velocity of a debris flow along the flow path, until the velocity decreases to zero. Using a Monte-Carlo and random walk approach reproduces trajectories that include the spreading effect of debris flows on fans (Gamma, 2000; Wichmann and Becht, 2003).

Overall, approx. 6.7 million trajectories were calculated over the entire area of Switzerland, representing the possible process space of debris flows. Each trajectory stands for a debris flow from the starting point to the outermost deposition point. Only debris flows in the channel were modelled. Unconfined debris flows on the slope (for example in alpine scree dumps) were categorized as landslide trajectories.

Landslide trajectories in SilvaProtect-CH consider shallow landslides (soil slips/spontaneous landslides) and hillslope debris flows. The landslide scars (starting zones) were modelled using the infinite slope model, where the slope stability is calculated for each grid cell. The infinite slope model is used to calculate a factor of safety (FS), based on limit equilibrium analysis that determines the balance between shear stress, which induces fracture along the supposed failure plane, and shear strength, which serves to resist shear fracture (Lee and Park, 2016; Selby, 1993). The decisive parameters are the slope inclination, which is calculated from the digital elevation model, the subsurface water level, and shear parameters (cohesion and friction angle) derived from the geotechnical map of Switzerland (Liener and Kienholz, 1998; Tobler et al., 2013a, 2013b).

Based on the modelled landslide scars, the possible flow path trajectories of shallow landslides were simulated. In order to keep the number of trajectories as low as possible, the raster cells of each landslide scar were thinned out before modelling the run-out distances. Based on the parameter set defined in test areas, the calculation of landslide scars and flow path trajectories was carried out automatically over the entire area of Switzerland. Due to the large landslide scars area, approx. 47.6 million landslide trajectories were calculated.

References cited:

Gamma, P., 2000. dfwalk – Ein Murgangsimulationprogramm zur Gefahrenzonierung. Geographica Bernensia, G66. Geographisches Institut der Universität Bern, 144 p. [in German].

Geiger, H., Röthlisberger, G., Stehli, A., Zeller, J., 1992. Extreme Punktregen unterschiedlicher Dauer und Wiederkehrperioden 1901-1970. Hydrol. Atlas der Schweiz.

Lee, J.H., Park, H.J., 2016. Assessment of shallow landslide susceptibility using the transient infiltration flow model and GIS-based probabilistic approach. Landslides 13, 885–903. doi:10.1007/s10346-015-0646-6

Liener, S., Kienholz, H., 1998. Predicting the spatial distribution of shallow landslides - the improved model SLIDISP, in: Buccianti, A., Nardi, G., Potenza, R. (Eds.),

Proceedings of the International Association for Mathematical Geology IAMG'98. Isola d'Ischia, Naples, pp. 229–234.

Perla, R., Cheng, T.T., McClung, D.M., 1980. A two-parameter model of snow-avalanche motion. J. Glaciol. 26, 197–207.

Quinn, P.F., Beven, K.J., Lamb, R., 1995. The in(a/tan/β) index: How to calculate it and how to use it within the topmodel framework. Hydrol. Process. 9, 161–182. doi:10.1002/hyp.3360090204

Rickenmann, D., 2005. Runout prediction methods, in: Jakob, M., Hungr, O. (Eds.), Debris-Flow Hazards and Related Phenomena. Praxis-Springer, Heidelberg, pp. 263–282.

Schneider, B., 1998. Geomorphologisch plausible Rekonstruktion der digitalen Repräsentation von Geländeoberflächen aus Höhenliniendaten. Universität Zürich.

Tobler, D., Riner, R., Pfeifer, R., 2013a. Runout Modelling of Shallow Landslides Over Large Areas with SliDepot, in: Margottini, C., Canuti, P., Sassa, K. (Eds.), Landslide Science and Practice. Springer Berlin Heidelberg, Berlin, Heidelberg, pp. 239–245. doi:10.1007/978-3-642-31310-3_32

Tobler, D., Riner, R., Pfeifer, R., 2013b. Modeling Potential Shallow Landslides over Large Areas with SliDisp+, in: Margottini, C., Canuti, P., Sassa, K. (Eds.), Landslide Science and Practice. Springer Berlin Heidelberg, Berlin, Heidelberg, pp. 37–45. doi:10.1007/978-3-642-31310-3_6

Wichmann, V., Becht, M., 2003. Modelling of geomorphological processes in an alpine catchment, in: 7th International Conference on GeoComputation. Southampton.

Zimmermann, M., Mani, P., Gamma, P., 1997. Murganggefahr und Klimaänderung – ein GIS-basierter Ansatz. vdf Hochschulverlag, Zürich.

SUPPLEMENTARY TABLES

Table S1: Characteristics of the 40 test catchments. Dominant recruitment process categories are: B = Bank erosion, D = Debris flow, I = Instream wood mobilization, L = Landslide

Stream/River	Date	Canton	LW volume [solid m^3]	Observation category	Dominant recruitment process	Catchment area [km^2]	Stream length [km]	Forested stream length [km]	Forest area [km^2]	Deciduous trees [%]	Peak discharge [m^3/s]	Return period [a]	Runoff volume [m^3]	Sediment load [m^3]	Melton ratio [-]	Precipitation duration [h]	Precipitation average [mm]
Chirel	22.08.2005	Berne	11350	Recruitment	D, B	128.7	134.8	72.1	30.1	24.2	100		5'414'123	90'000	0.17		101
Grosse Melchaa	22.08.2005	Obwalden	5530	Recruitment	L, B, D	72.6	110.6	61.3	16.1	47.6			9'362'585	125'000	0.26		226
Kleine Emme	22.08.2005	Lucerne	5350	Recruitment	B	478.4	1518.2	1149.8	180.1	31.4					0.09		
Landquart	22.08.2005	Grisons	4140	Recruitment	B, (L)	119.0	148.1	11.2	6.1	14.4	150		6'725'221	200'000	0.19	72	150
Chiene	22.08.2005	Berne	3150	Recruitment	D, B, L	90.5	116.0	50.8	16.2	24.1	90	50-100	6'135'402	90'000	0.31		162
Holdenbach	18.09.2006	Uri	3000	Deposition	B, I, (M)	5.4	11.6	6.8	1.2	28.4				12'000	0.71		
Ava da Tuors	08.08.2009	Grisons	2310	Deposition	D	56.8	85.7	20.0	5.0	7.3					0.28	2	29
Horboden	22.08.2005	Berne	2261	Recruitment	D, B, (I)	28.6	28.966	16.5	5.7	29.6					0.34		
Schächen	22.08.2005	Uri	2000	Deposition	D, L, B, I	108.0	129.3	60.9	18.1	32.6	120		6'992'233	200'000	0.27	48	245
Chratzmattigrabe	22.08.2005	Berne	2000	Recruitment	D	3.1	3.9	3.1	0.6	28.7			131'782	30'000	0.91		135
Engelberger Aa	22.08.2005	Nidwalden	1875	Deposition		229.0	296.0	142.0	48.3	46.4	230	200	28'997'813	210'000	0.18	48	186
Ticino - Airolo	25.08.1987	Ticino	1824	Deposition	B	156.0	18.8	6.5	19.0	15.3	210		8'000'000		0.09		
Fildrich	22.08.2005	Berne	1689	Recruitment	B	19.8	14.594	6.5	3.5	30.2					0.33		
Engstlige	10.10.2011	Berne	1200	Deposition	B, I	145.0	246.9	116.9	23.6	25.9	115		3'246'811	20'000	0.21	16	68
Zulg	04.07.2012	Berne	1000	Deposition	B, L, I	88.2	298.0	247.7	35.0	25.1	210	100		15'000	0.16	2.5	60
Steinibach (Dorfbach)	15.08.1997	Obwalden	900	Deposition	I, D	3.3	4.2	3.0	1.7	37.4	40	100		26'000	0.85	2.5	140
Goldbach	22.08.2005	Berne	888	Recruitment	B, I	3.8	3.862	2.8	0.7	24.7					0.85		
Chratzmattigrabe	23.08.2005	Berne	748	Deposition	D	3.1	3.9	3.1	0.6	28.7			131'782	30'000	0.91		135
Buembachgrabe	24.07.2014	Berne	717	Recruitment	B, L	4.9	4.6	3.9	1.4	16.4	59				0.51		97
Ganterbach / Saltina	24.09.1993	Valais	705	Recruitment	B, L	66.5	101.9	32.9	16.0	8.8	85	50	1'350'000	250'000	0.33		
Schöniseibach	24.07.2014	Berne	641	Recruitment	B, L	4.5	1.5	1.3	0.7	13.8	55				0.55		81
Laui	31.05.2017	Obwalden	600	Deposition	B, L, I	44.8	149.8	121.3	25.0	34.2	90	30-50		10000	0.24	1	100
Chlosegrabe	22.08.2005	Berne	542	Recruitment	D	3.1	4.185	3.1	0.5	23.6					0.83		
Secklisbach	01.08.2005	Nidwalden	510	Deposition	L	24.2	35.3	15.2	4.4	28.0	80	100		60'000	0.41		
Sädelgrabe	24.07.2014	Berne	490	Deposition	L, B, D	1.3	2.0	2.0	0.3	23.9	30	300		17'000	0.97	7	96
Steinibach (Giswil)	09.06.1996	Obwalden	450	Deposition	I, D, B	12.0	10	8.0	5.4	24.5	50	> 100	45'000	200'000	0.41	2	
Rütigrabe	22.08.2005	Berne	339	Recruitment	D	1.8	2.574	1.7	0.4	27.8					1.14		

Maienbach	15.08.1997	Obwalden	300	Deposition	D	4.9	8.5	7.1	1.5	36.6	35	<100		13'500	0.74	2.5	120
Isentalerbach	22.08.2005	Uri	300	Deposition	D	59.7	63.3	29.8	12.7	44.6			6'247'710	10'000	0.32		106
Haldibach	22.08.2005	Nidwalden	300	Deposition	D, L	2.9	4.1	2.7	1.0	18.2			309'636	250'000	0.82	48	163
Gärtelbach	24.07.2014	Berne	260	Deposition	D, B	0.8	1.7	1.7	0.2	24.2	18	300		8'000	1.18	7	96
Goldach	01.06.2009	Thurgau	240	Deposition		50.4	140.9	125.5	15.9	49.2					0.12		
Varuna	18.07.1987	Grisons	180	Recruitment	B, L	4.0	5.1	1.7	1.2	8.8	2		64'800	200'000	1.20		
Pletschenbächli	22.08.2005	Berne	174	Recruitment	D	2.2	5.001	1.9	0.3	18.3					0.85		
Gruonbach	22.08.2005	Uri	165	Recruitment	L, D	8.3	16.4	14.7	4.1	16.9			773'867	40'000	0.62		115
Schwendibach	24.08.2005	Berne	150	Deposition	D	11.1	25.3	8.1	2.0	9.1	60			11'000	0.55	65	275
Goneri (Gerewasser)	24.09.1993	Valais	145	Recruitment	I	40.0	61.9	7.0	1.6	16.8					0.29		
Bärselbach	24.07.2014	Berne	141	Recruitment	B, L	13.1	7.0	6.3	3.5	17.0	108				0.31		92
Saxetebach	03.07.1987	Berne	135	Deposition	B	20.0	8.3	4.6	7.0	36.8					0.49		
Sundgraben	02.01.2012	Berne	45	Deposition	L, (D)	9.7	23.4	22.2	5.1	22.5	250	30		40'000	0.48	115	61

Table S2: Mean channel width extrapolation of the ecomorphological dataset based on stream order (FLOZ) and altitude classes.

		Altitude [m a.s.l.]							
		<600		600-1200		1200-1800		>1800	
		Average stream width [m]	Total stream length [km]	Average stream width [m]	Total stream length [km]	Average stream width [m]	Total stream length [km]	Average stream width [m]	Total stream length [km]
Stream order	FLOZ 1	1.2	2641	1.3	3973	2.3	1163	5.1	431
	FLOZ 2	1.8	2100	2.1	2493	3.9	872	8.2	278
	FLOZ 3	3.2	1811	4.2	1575	7.3	590	11.0	259
	FLOZ 4	5.1	1229	9.3	1107	15.9	578	17.2	182
	FLOZ 5	13.1	694	17.3	901	22.6	301		
	FLOZ 6	17.4	563	27.3	404	24.2	20		
	FLOZ 7	29.4	500	42.0	80				
	FLOZ 8	70.9	341						
	FLOZ 9	82.7	247						

SUPPLEMENTARY FIGURES

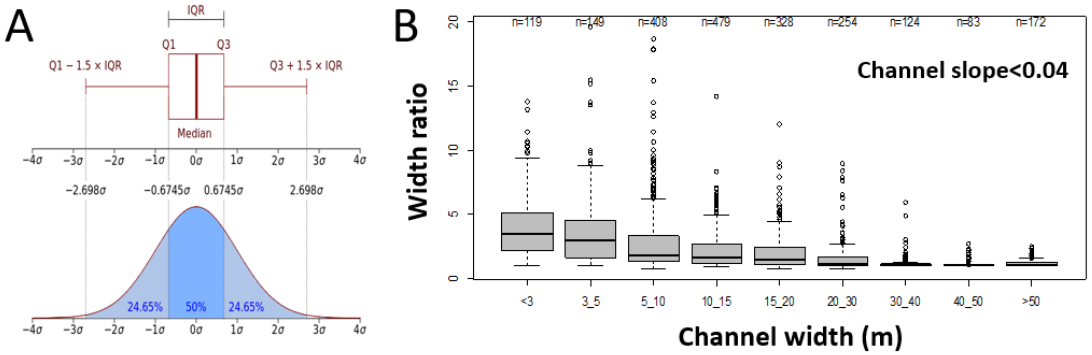

C

width/ width ratio	<3	3_5	5_10	10_15	15_20	20_30	30_40	40_50	>50
Medium (Q1)	1.2	1.1	1.1	1.1	1.1	1	1	1	1
Large (median)	3	2	2	2	2	1.6	1.3	1.2	1.2
Very large (Q3)	4	3	2.5	2.5	2.2	1.8	1.6	1.5	1.5

Figure S1: (A) Boxplot and density function showing the quartiles used to define the scenarios; (B) boxplots of width ratio values for different channel width classes for rivers with longitudinal slopes lower than 4%; (C) table showing the final values of width ratio used for the three scenarios and the different width classes.

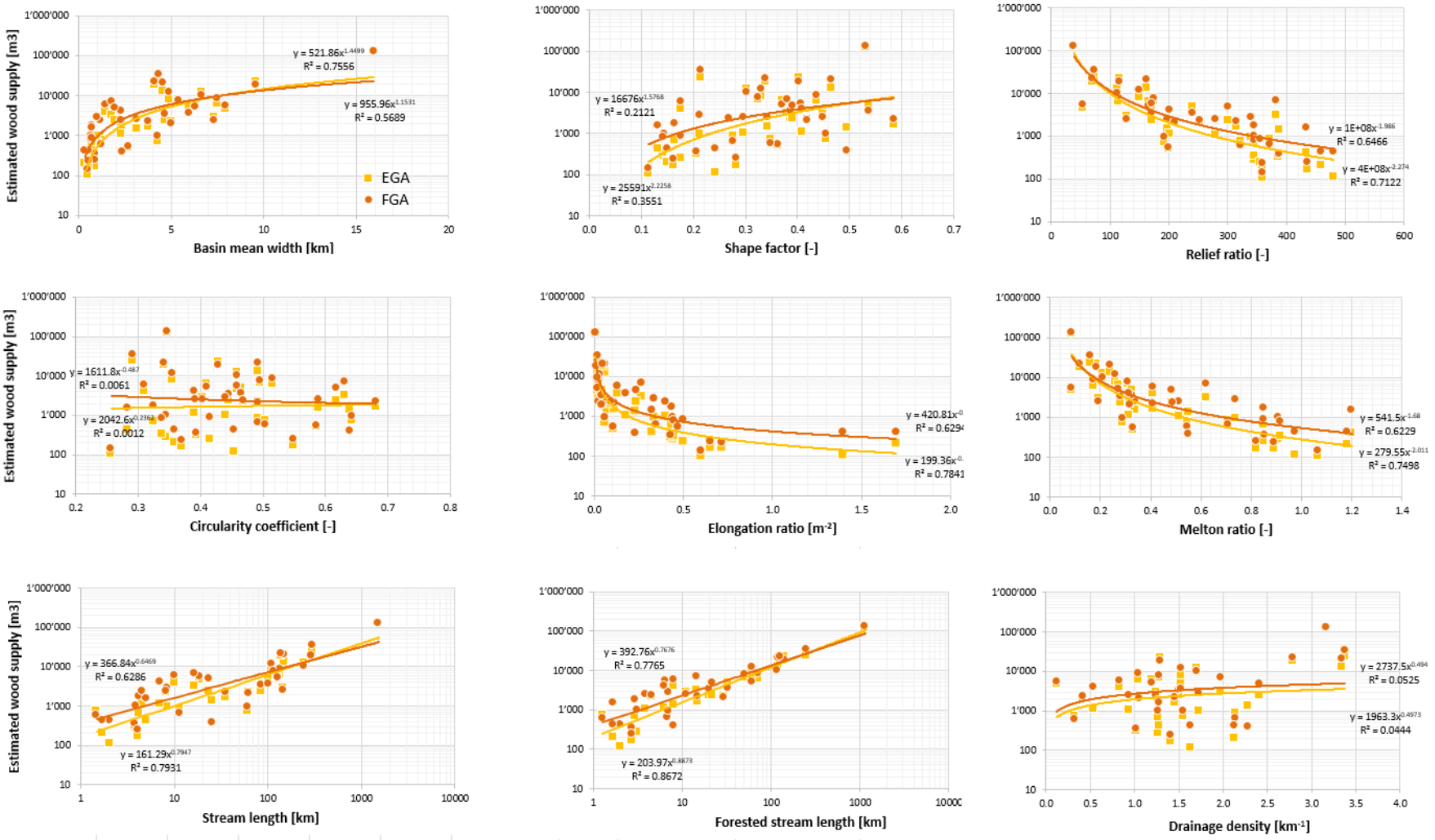

Figure S2: Wood volume estimated (large scenario) by the two models and different catchment characteristics: basin mean width, shape factor, relief ratio, circularity coefficient, elongation ratio, Melton ratio, stream length, forested stream length, drainage density.

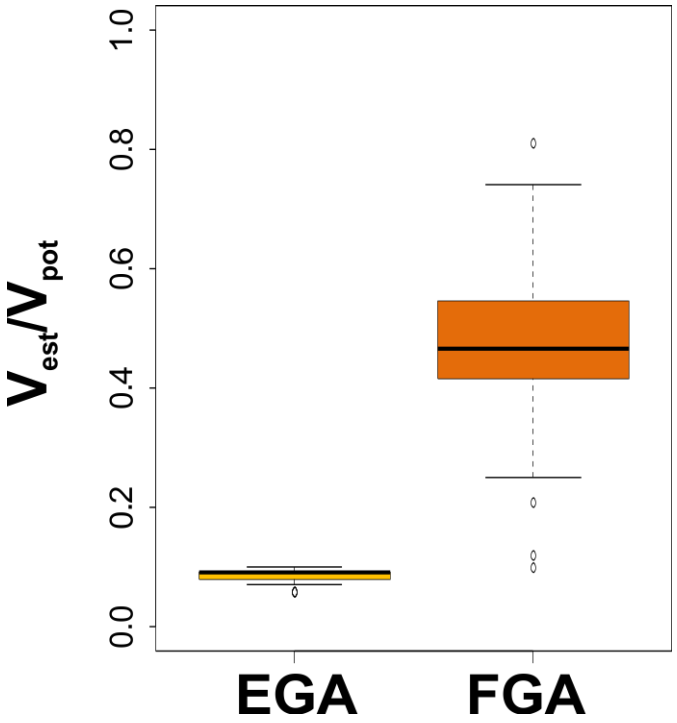

Figure S3: Boxplots for the ratio of estimated and potential wood supply volumes (large scenario) calculated for EGA (dark grey) and FGA (light grey) for all sites.

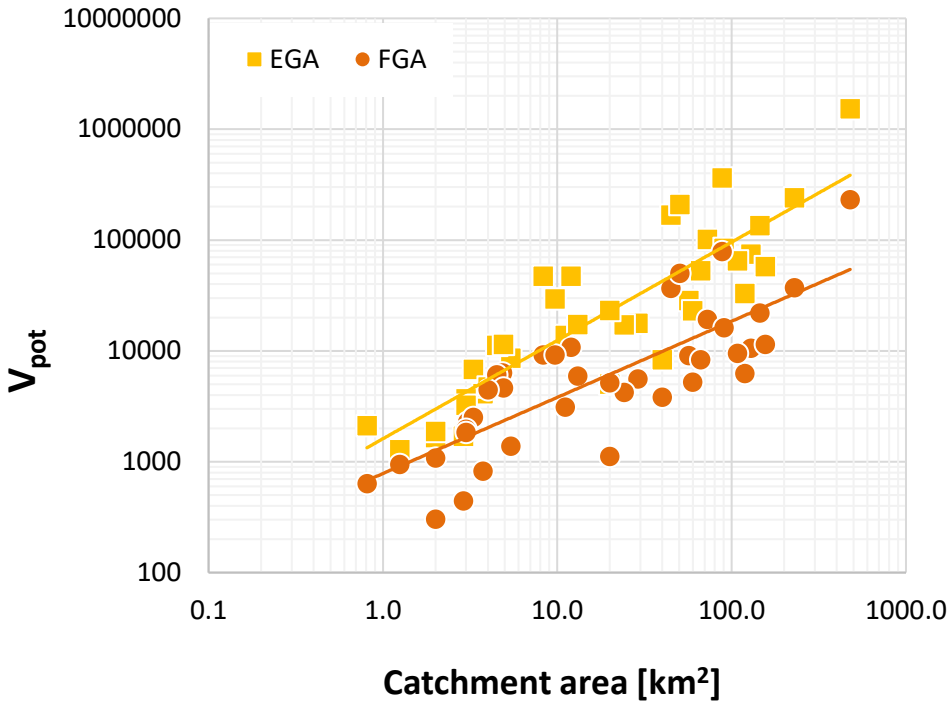

Figure S4: Scatter plot showing potential LW supply volume (large scenario) by the two models in relation to the respective catchment area.

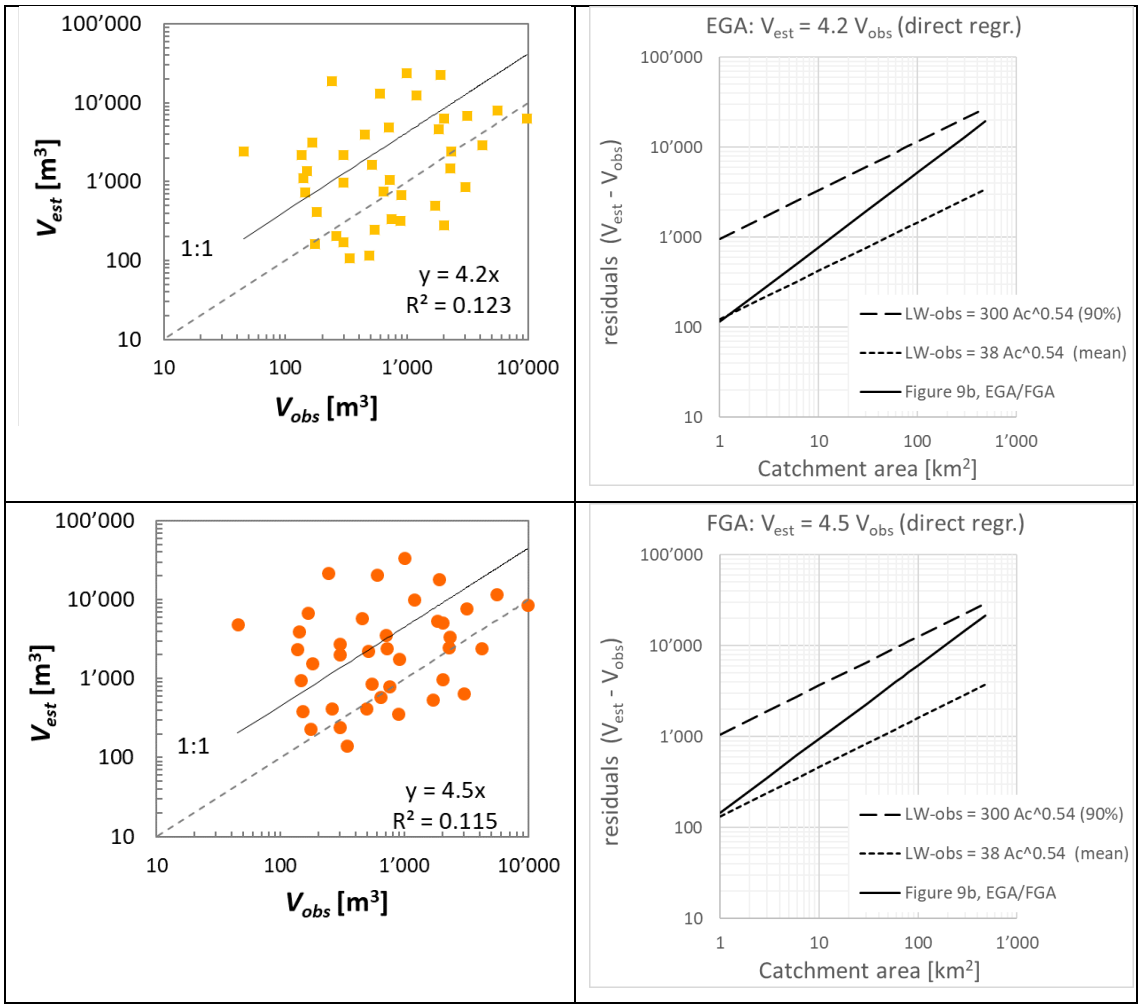

Figure S5: Top row left: Linear regression of V_{est} and V_{obs} for EGA. Top row right: Residuals (V_{est} - V_{obs}) for EGA in comparison with empirical LW estimation formulas (50 and 90% percentile) depending on catchment area. Bottom row left: Linear regression of V_{est} and V_{obs} for FGA. Bottom row right: Residuals (V_{est} - V_{obs}) for FGA in comparison with empirical LW estimation formulas (50 and 90% percentile) depending on catchment area.